TWO DIMENSIONAL VIBRATIONAL SPECTROSCOPY OF ANTAMANIDE; A SIMULATION STUDY

S. M. PARK, C. SCHEURER, AND S. MUKAMEL
Department of Chemistry, University of Rochester, Rochester, NY 14627, USA
E-mail: mukamel@chem.rochester.edu

Abstract

Infrared pulse sequences may be used to provide ultrafast snapshots of molecular structural fluctuations. The two-dimensional (2D) vibrational echo and reverse transient grating signals from the amide I band of the four conformational states of the cyclic decapeptide antamanide are computed. We demonstrate that by combining a method of calculating the vibrational Hamiltonian from MD snapshots, a clustering algorithm for structures, and the nonlinear exciton equations (NEE) it is possible to simulate realistic multidimensional IR spectra of chemically and biologically interesting systems.

1 Introduction

The cyclic decapeptide antamanide [-V1–P2–P3–A4–F5–F6–P7–P8–F9–F10-] (Fig. 1) is a small oligopeptide which serves as a model for proteins and was studied intensively by NMR as well as theoretically by MD simulations (see[1] and references therein). Antamanide has biological activity as an antidote against the poisonous phalloidins that occur in the mushroom *Amanita phalloides*.[2] Remarkably, antamanide is contained in small quantities in the same mushroom. In mammals, phalloidins block the depolymerization of F–actin into G–actin in the liver cell membrane. This process can be prevented by the presence of antamanide.

Antamanide contains a network of intramolecular hydrogen bonds[3,4] (Fig. 1 b, c). It has been suggested, initially from 1 D NMR measurements[5] and subsequently from ultrasonic absorption,[6] that it exists in solution in an equilibrium of rapidly interchanging conformers ($k \approx 10^6\, s^{-1}$). In more recent studies, two–dimensional NMR, relaxation measurements in the rotating frame, and homo– and heteronuclear coupling constant determinations have been used to characterize the dynamic properties of the molecule.[4] Direct evidence for the presence of a conformational exchange process with an activation energy of $\approx 20\,\mathrm{kJ\,mol^{-1}}$ and an exchange lifetime of $\approx 25\,\mu\mathrm{s}$ at 320 K has been obtained from rotating frame relaxation $T_{1\rho}$ measurements which suggest rapid hydrogen bond exchange dynamics at ^{1}Val HN and ^{6}Phe HN.

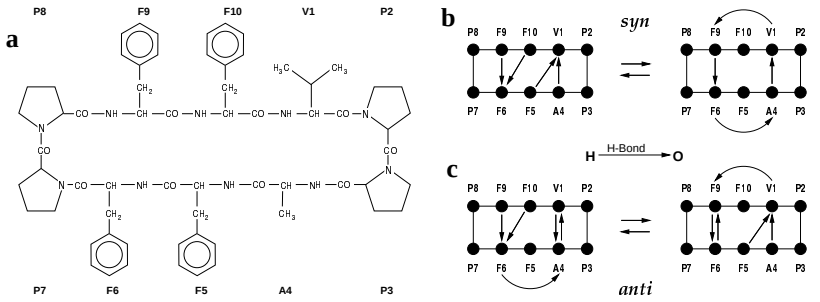

Figure 1. **a** The cyclic decapeptide antamanide. **b** Schematic representation of the hydrogen bonding network in the structural *syn*–pair (E 116, G 129) of the antamanide exchange system. **c** Schematic representation of the hydrogen bonding network in the structural *anti*–pair (A 128, G 193) of the antamanide exchange system.

Local backbone dihedral angle changes accompany these processes. Two of the most likely pairs of dynamic exchange systems have been identified, designated as the *syn*–pair (Fig. 1 b) and the *anti*–pair (Fig. 1 c) on the basis of the *syn*–correlated and *anti*–correlated structural changes at the two mentioned residues.[4] It was pointed out that even though the two preferred exchange systems which emerged from the analysis led to the best fit of the available experimental data, further pair structures could not be excluded for antamanide in solution. Further measurements would be necessary to characterize the ensemble of possible structure in more detail.

Multidimensional nonlinear optical experiments which are able to probe the respective dynamics in real-time and not indirectly via relaxation measurements as in NMR could complement these NMR studies. Two–dimensional IR spectroscopy of the amide I band proved to be sensitive to hydrogen bonding involving the carbonyl oxygen.[7–9] This band originates from the stretching motion of the C=O bond coupled to the bending of the N-H bond and the stretching of the C-N bond (see Fig. 2).[10] Conformers of the decapeptide with differing hydrogen bond networks should give rise to different 2D–spectra that allow the experimental identification of the species in solution.

In addition to hydrogen bond dynamics, sidechain dynamics,[11] backbone dynamics,[12] and proline ring puckering[1,13,14] in antamanide were studied by NMR relaxation measurements as well as by MD simulations. The study of sidechain dynamics was performed on the four phenylalanine sidechains[11] (see Fig. 3 a). Based on a MD trajectory a motional model for the angular degrees of freedom (χ_1, χ_2 in Fig. 3 b) was proposed. The analytical model describes

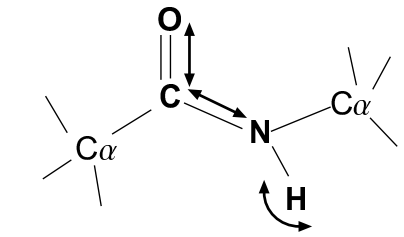

Figure 2. Schematic representation of a peptide bond in proteins. The arrows denote the stretching motion of the C=O bond coupled to the stretching of the C-N bond and the bending of the N-H bond, thereby contributing to the amide I band .

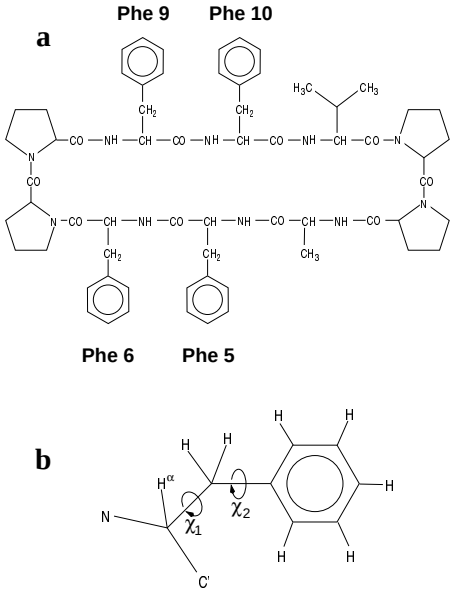

Figure 3. **a** The four phenylalanine sidechains in the cyclic decapeptide antamanide. **b** Rotational degrees of freedom of the phenylalanine sidechains.

Gaussian axial fluctuation (GAF) within localized potential wells, interrupted by occasional jumps between different rotameric states over relatively high barriers. The relevant motional parameters like jump rates and fluctuation amplitudes were extracted by fitting a large set of NMR relaxation data for the different sidechains to the analytical model.

Pump–probe and optical fluorescence spectroscopy can directly probe the dynamics of the phenylalanine chromophores in real–time.[15] The validity of the dynamical model obtained from NMR relaxation studies could be tested and the respective motional parameters determined. NMR and optical spectroscopy can give complementary information on the dynamics and allow a

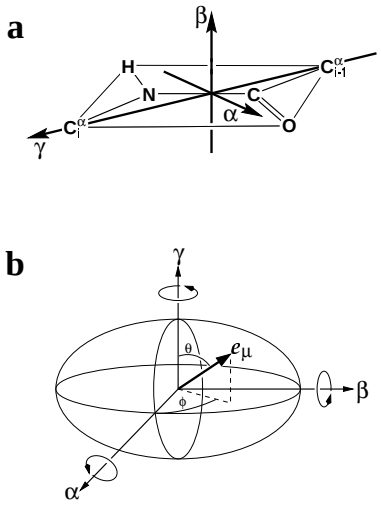

Figure 4. **a** Definition of the local reference coordinate system for the description of anisotropic motion of the peptide planes in proteins. **b** Fluctuation ellipsoid describing anisotropic intramolecular motion.

cross–validation of the models derived from experimental data.

An extension of the GAF model to three dimensions has been used to describe the anisotropic peptide–plane motion in the backbone.[12] The model describes the reorientation in terms of rotations of the mostly rigid peptide plane about the three axes α, β, and γ (see Fig. 4 a) with Gaussian fluctuations about an average angle. The fluctuation amplitudes can be visualized in form of reorientational fluctuation tensors (Fig. 4 b). Fitting of the motional model to a set of ^{13}C' T_1, ^{15}N T_1, and $\{^1H\}^{15}$N NOE values resulted in motional parameters for the six non–proline peptide planes.

Multidimensional IR spectroscopy of the amide I band provides an independent observation of the same fast dynamics which is free of the assumptions underlying the interpretation of NMR relaxation data. The determination of the set of peptide planes in a protein that can be described by fast small–amplitude motion is important for the identification of the peptide groups involved in large–amplitude motions that dominate the conformational changes of the protein underlying its biological function. Only after a sound understanding of the small–amplitude motion and its separation from dynamics leading to conformational changes is achieved, it shall be possible to develop motional models for the more complex large-amplitude motions.

Different visible or IR nonlinear spectroscopic techniques can cover the whole range of relevant timescales (from ps to μs) occuring in the dynamics of Antamanide.[15,16] Comparison with the more indirect NMR relaxation

experiments should lead to a better understanding of the relevant dynamical processes in this model compound. Detailed motional models can thereby be tested with completely independent experimental methods. The improved understanding of the dynamics in a small model compound should facilitate investigations on larger proteins and help to identify limitations and strengths of either spectroscopic technique.

2 Molecular Dynamics Simulation

The advent of femtosecond laser pulses has made it possible to apply various multidimensional spectroscopic techniques to probe electronic and vibrational dynamics on the femtosecond timescale. Spectroscopic techniques based on the application of sequences of carefully shaped and timed femtosecond pulses provide a multidimensional view of molecular structure as well as vibrational and electronic motions, interactions, and relaxation processes.[17–29] For example, the intensities and profiles of cross-peaks give a direct signature of molecular structure (distances between chromophores) and dynamics (the spectral density of the chromophores' environments). By combining MD simulation, a fluctuating exciton Hamiltonian for the amide-I band [reference], and the NEE approach[29,30] for the calculation of 2D vibrational spectra 2D vibrational echo signals of the cyclic decapeptide antamanide was calculated. For the MD simulation, the dihedral angles of four most common conformers (E116, G129, A128, and G193) were used to construct antamanide using the CHARMM 27 force field, topologies, and parameters. For each structure constructed, SHAKE algorithm[31] was applied to constrain bond lengths, and Adopted Basis Newton-Raphson (ABNR) algorithm was used to minimize the energy. After equilibration in CHARMM a 50 nanosecond Langevin dynamics MD trajectory with a timestep of 1 femtosecond was generated for each structure, and snapshots of the structure were taken every 2 picosecond. 25,000 snapshots of antamanide have been obtained for each conformer. Bath temperature for the MD simulation was set at 300 K and closely monitored for any abrupt fluctuation; each simulation was completed successfully with a temperature variation of less than, or equal to ± 10 K from the set value. Solvent was not included explicitely in the simulation, instead the stochastic models for force - Langevin dynamics- was applied to antamanide to simulate the environment of chloroform.

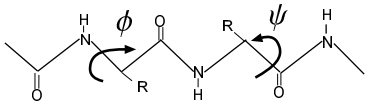

Figure 5. Schematic illustration of the protein backbone dihedral angles ϕ and ψ

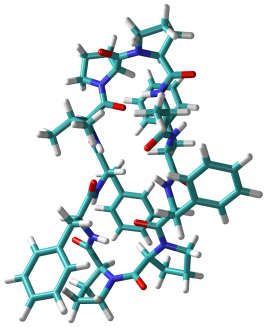

Figure 6. 3D representation of Antamanide

3 The Clustering Algorithm

We have used a clustering algorithm, written in C, to classify each structure generated by the simulation into a cluster of either E116, G129, A128, or G193. The input for the algorithm is the coordinate information from the MD simulation snapshot. The output shows which cluster the snapshot belongs to and lists the fluctuations of the transition frequencies and dipole-dipole couplings. It consists of following steps:

1. The backbone dihedral angles ϕ and ψ are measured for each residue (see Fig. 5).

2. Hydrogen bond energy is calculated using Kabsch-Sander electrostatic energy criterion[32] in which $f = 332\, e^{-2}\, \mathring{A}$ kcal/mol, $q_1 = 0.42\, e$, and $q_2 = 0.2\, e$.

$$E_{ks} = f q_1 q_2 \left(\frac{1}{d_{ON}} + \frac{1}{d_{CH}} - \frac{1}{d_{CN}} - \frac{1}{d_{OH}}\right) \tag{1}$$

   - A hydrogen bond is deemed to exist if $E_k s$ gives a value less than the cutoff - 0.5 kcal/mol.
   - The two strongest H-bonds per acceptor Oxygen are determined.

3. The mean square deviation of ϕ, ψ, and hydrogen bond energy is calculated with respect to E116, G129, A128 and G193 (see Fig. 1 b,c).

4. The snapshot is put into one of the four cluster which showed the smallest mean square deviation.

4 The Fluctuating Vibrational Exciton Model

Antamanide is modelled as a system of $N = 10$ interacting local vibrations representing the 10 peptide bonds (see Fig. 7). For third-order spectroscopies, only the lowest three levels of each peptide group need to be taken into consideration.[9,33]

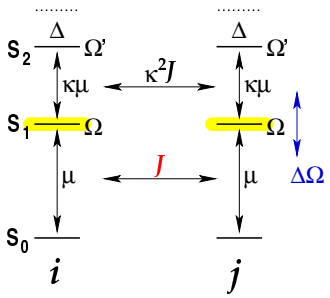

Figure 7. The three-level systems representing the peptide plane groups in the exciton Hamiltonian. The levels in each system, i and j, are denoted S_0, S_1, S_2 with energies $0, \Omega, \Omega'$ for each chromophore. ($\Delta = \Omega' - 2\Omega$) The levels are shifted by hydrogen bonds to the carbonyl oxygen giving rise to a fluctuating term $\Delta\Omega$. The only nonvanishing elements of the transition dipole operator are μ and $\mu' = \kappa$. The carbonyl vibrations are dipole-coupled where the coupling matrix J_{ij} depends on the local geometries.

In the present MD simulation, only the fluctuations of transition frequencies (Ω_i) and dipole-dipole couplings (J_{ij}),[34] which are expected to dominate the spectra, are taken into account in computing the Hamiltonian. Fluctuations of other parameters, such as the dipole coupling to the laser field are neglected. The quadratic part of the Hamiltonian can be represented in the form of coupled harmonic oscillator:[9]

$$\hat{H}_0 = \sum_i \epsilon_i B_i^\dagger B_i + \sum_{i \neq j} J_{ij} B_i^\dagger B_j \qquad (2)$$

The transition dipole-dipole coupling constant between each residues (J_{ij}) is given by:[9]

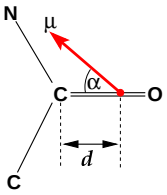

$$J_{ij} = \frac{1}{r_{ij}^3}(\vec{\mu}_i \cdot \vec{\mu}_j - 3(\vec{n}_{ij} \cdot \vec{\mu}_i)(\vec{n}_{ij} \cdot \vec{\mu}_j) \qquad (3)$$

in which $\alpha = 25°$, $|\mu| = 0.37\,\mathrm{D}$, $d = 0.868\,\text{Å}$. The fluctuation in the vibrational frequencies induced by the hydrogen bond of carbonyl group (C_i) to NH groups of different residues (NH_j) is given by:

$$\delta\epsilon_i = \alpha_H(2.6 - d_{OH}) \qquad (4)$$

Here d_{OH} is the O$\cdots$H distance in Å and the vlaue of $\alpha_H = -30\,\mathrm{cm}^{-1}/\text{Å}$ results in a frequency downshift of $\sim 20\,\mathrm{cm}^{-1}$ for a typical hydrogen bond length of $1.9 - 2.0\,\text{Å}$.[7,35]

5 2D Vibrational Echo and Transient Grating Spectra

The lowest-order nonlinear IR spectroscopy in non-centrosymmetric media requires three pulses (see Fig. 8).[36] In femtosecond 2D three-pulse techniques, two of the three pulses are time-coincident and only differ by their wave vector k.[33]

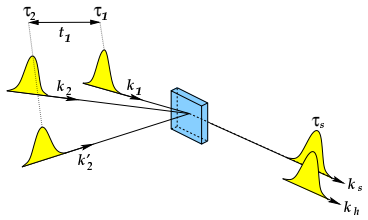

Figure 8. Nonlinear IR spectroscopy (photon echo technique)

The system interacts with a single pulse with wave vector k_1 at time τ_1 and twice with the pulses of a pulse pair $\mathbf{k_s} = \mathbf{k_2'} + \mathbf{k_2} - \mathbf{k_1}$ (photon echo), $\mathbf{k_s} = -\mathbf{k_2'} + \mathbf{k_2} - \mathbf{k_1}$ (reverse transient gating) at $t = \tau_2$. The delay between the single pulse and the pulse pair will be denoted $t_1 = \tau_2 - \tau_1$. The centered signal is detected by combining it with an additional heterodyne pulse k_h at time τ_s. This gives the second time variable $t_2 = \tau_s - \tau_2$ of the 2D correlation plot.

Closed expressions for the third–order nonlinear response function $R(t, \tau_3, \tau_2, \tau_1)$ were obtained in Ref.[30] by solving the Nonlinear Exciton Equations (NEE) for the exciton Hamiltonian. These can be used to obtain expres-

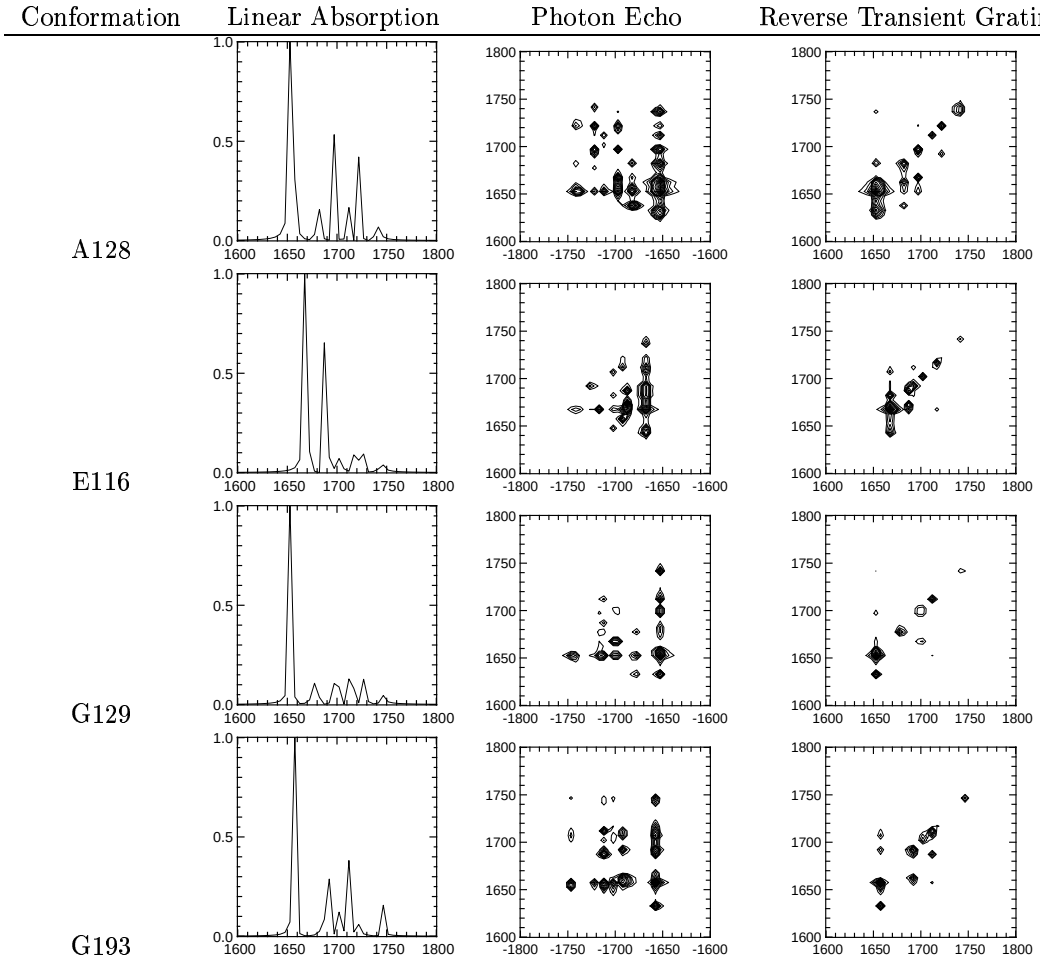

Figure 9. Signal intensities are given in arbitrary units. Frequencies are in cm^{-1}. Transition frequencies are between $1682 - 1736\,cm^{-1}$ for A128, $1700 - 1735\,cm^{-1}$ for E116, $1686 - 1735\,cm^{-1}$ for G129, and $1685 - 1738\,cm^{-1}$ for G193. Fluctuations in the transition frequencies of hydrogen bonded CO groups are between $5 - 24\,cm^{-1}$

sions for 2D signals $S(\Omega_2, \Omega_1)$ for different spectroscopies.[37] Double Fourier transformation of the time domain signal yields the signal in the frequency

domain

$$S(\Omega_2, \Omega_1) = \int_0^\infty dt_2 \int_0^\infty dt_1 \exp\left(i\left(\Omega_1 t_1 + \Omega_2 t_2\right)\right) S(t_2, t_1)$$

Figure 9 shows the linear absorption, photon echo and reverse transient grating spectra of a single snapshot from A128, E116, G129, and G193. All four linear absorption spectra show a peak with maximum intensity at $1650\,\mathrm{cm}^{-1}$ and other smaller peaks that is due to the amide I band absorption. Unlike the linear absorption, the photon echo and reverse transient grating spectra not only show diagonal peaks at $1650 - 1650\,\mathrm{cm}^{-1}$ but several off-diagonal peaks that provide characteristic signatures for each conformation. The average over an ensemble of spectra needs to be carried out in order to compare with experiment

Acknowledgements

The support of the National Institutes of Health (GM59230–01A2). C.S. thanks the Alexander von Humboldt Foundation for a Feodor Lynen fellowship.

References

1. J. W. Peng, C. A. Schiffer, P. Xu, W. F. van Gunsteren, and R. R. Ernst. Investigations of peptide hydration using NMR and molecular dynamics simulations: A study of effects of water on the conformation and dynamics of antamanide. *J. Biol. NMR*, 8:453–476, 1996.
2. T. Wieland and H. Faulstich. Amatoxins, phallotoxins, phallolysin, and antamanide — biologically–active components of poisonous amanita mushrooms. *Crit. Rev. Biochem.*, pages 185–260, 1978.
3. Rafael Brüschweiler, Martin Blackledge, and Richard R. Ernst. Multi–conformational peptide dynamics derived from NMR data: A new search algorithm and its application to antamanide. *J. Biol. NMR*, 1:3–11, 1991.
4. Martin Blackledge, Rafael Brüschweiler, Christian Griesinger, Jürgen M. Schmidt, Ping Xu, and Richard R. Ernst. Conformational backbone dynamics of the cyclic decapeptide antamanide. application of a new multiconformational search algorithm based on NMR data. *Biochemistry*, 32:10960–10974, 1993.
5. D. J. Patel. Antamanide conformations in non–aqueous media dependence on hydrogen–bond acceptor properties of solvent. *Biochemistry*,

12:667–676, 1973.
6. W. Burgermeister, T. Wieland, and R. Winkler. Antamanide — relaxation study of conformational equilibria. *Eur. J. Biochem.*, 44:311–316, 1974.
7. H. Torii, T. Tatsumi, and M. Tasumi. Effects of hydrogen bonding and solvation in dielectric media on the amide I frequencies: Ab initio molecular orbital study. *Mikrochim. Acta Suppl.*, 14:531–533, 1997.
8. P. Hamm, M. H. Lim, and R. M. Hochstrasser. Structure of the amide I band of peptides measured by femtosecond nonlinear–infrared spectroscopy. *J. Chem. Phys. B*, 102:6123–6138, 1998.
9. C. Scheurer, A. Piryatinski, and S. Mukamel. Signatures of β–peptide unfolding in two–dimensional vibrational echo spectroscopy: A simulation study. *J. Am. Chem. Soc.*, 123(13):3114–3124, 2001.
10. Samuel Krimm and Jagdeesh Bandekar. Vibrational spectroscopy and conformation of peptides, polypeptides, and proteins. *J. Adv. Protein Chem.*, 38:181–364, 1986.
11. Tobias Bremi, Rafael Brüschweiler, and Richard R. Ernst. A protocol for the interpretation of side–chain dynamics based on NMR relaxation: Application to phenylalanines in antamanide. *J. Am. Chem. Soc.*, 119:4272–4284, 1997.
12. Tobias Bremi and Rafael Brüschweiler. Locally anisotropic internal polypeptide backbone dynamics by NMR relaxation. *J. Am. Chem. Soc.*, 119:6672–6673, 1997.
13. Z. L. Madi, C. Griesinger, and R. R. Ernst. Conformational dynamics of proline residues in antamanide. j coupling analysis of strongly coupled spin systems based on E.COSY spectra. *J. Am. Chem. Soc.*, 112:2908–2914, 1990.
14. Jürgen M. Schmidt, Rafael Brüschweiler, Richard R. Ernst, Roland L. Dunbrack, Diane Joseph, and Martin Karplus. Molecular dynamics simulation of the proline conformational equilibrium and dynamics in antamanide using the charmm force field. *J. Am. Chem. Soc.*, 115:8747–8756, 1993.
15. T. Elsaesser, S. Mukamel, M. M. Murnane, and N. F. Scherer, editors. *Ultrafast Phenomena XII*, Berlin, 2001. Springer.
16. S. Mukamel and R. Hochstrasser. *Chemical Physics (Special Issue)*, 266(2–3):135, 2001.
17. M. C. Asplund, M. T. Zanni, and R. M. Hochstrasser. Two-dimensional infrared spectroscopy of peptides by phasecontrolled femtosecond vibrational photon echoes. *Proc. Nat. Acad. Sci.*, 97:8219–8224, 2000.
18. R. Zadoyan and V. A. Apkarian. Imaging the molecular rovibrational co-

herence through time-gated, frequency-resolved coherent anti-stokes raman scattering. *Chem. Phys. Lett.*, 326:1–10, 2000.
19. K. A. Merchant, David E. Thompson, and M. D. Fayer. Two–dimensional time–frequency ultrafast infrared vibrational echo spectroscopy. *submitted*, 2000.
20. P. Hamm, M. Lim, W. DeGrado, and R. Hochstrasser. Pump/probe self heterodyned 2D spectroscopy of vibrational transitions of a small globular peptide. *J. Chem. Phys.*, 112:1907–1916, 2000.
21. K. Okumura, A. Tokmakoff, and Y. Tanimura. Structural information from two-dimensional fifth–order raman spectroscopy. *J. Chem. Phys.*, 111(2):492–503, 1999.
22. K. D. Rector, A. S. Kwok, C. Ferrante, A. Tokmakoff, C. W. Rella, and M. D. Fayer. Vibrational anharmonicity and multilevel vibrational dephasing from vibrational echo beats. *J. Chem. Phys.*, 106:10027–10036, 1997.
23. T. H. Joo, Y. W. Jia, J. Y. Yu, D. M. Jonas, and G. R. Fleming. Dynamics in isolated bacterial light harvesting antenna (LH2) of rhodobacter sphaeroides at room temperature. *J. Phys. Chem.*, 100:2399–2409, 1996.
24. E. J. A. Brown, I. Pastirk, B. I. Grimberg, V. V. Lozovoy, and M. Dantus. Population and coherence control by three-pulse four-wave mixing. *J. Chem. Phys.*, 111:3779–82, 1999.
25. John D. Hybl, Yannick Christophe, and David M. Jonas. Peakshapes in femtosecond 2D correlation spectroscopy. *Chem. Phys.*, 266:295–309, 2001.
26. O. Golonzka, M. Khalil, N. Demirdöven, and A. Tokmakoff. Vibrational anharmonicities revealed by coherent two-dimensional infrared spectroscopy. *Phys. Rev. Lett.*, 86(10):2154–2157, 2001.
27. M. Khalil and A. Tokmakoff. Signatures of vibrational interactions in coherent two–dimensional infrared spectroscopy. *Chem. Phys.*, 266:213–230, 2001.
28. K. A. Merchant, David E. Thompson, and M. D. Fayer. Two-dimensional time-frequency ultrafast infrared vibrational echo spectroscopy. *Phys. Rev. Lett.*, 86(17):3899–3902, 2001.
29. S. Mukamel. Multidimensional femtosecond correlation spectroscopies of electronic and vibrational excitations. *Annu. Rev. Phys. Chem.*, 51:691–729, 2000.
30. V. Chernyak, W. M. Zhang, and S. Mukamel. Multidimensional femtosecond spectroscopies of molecular aggregates and semiconductor nanostructures; the nonlinear exciton equations. *J. Chem. Phys.*, 109:9587, 1998.
31. J. P. Ryckaert, G. Ciccotti, and H. J. C. Berendsen. Numerical integra-

tion of the cartesian equations of motion of a system with constraints: molecular dynamics of n-alkanes. *J. Comp. Phys.*, 23:327–341, 1977.
32. W. Kabsch and C. Sander. Dictionary of protein secondary structure: pattern recognition of hydrogen-bonded and geometrical features. *Biopolymers*, 22:2577–2637, 1983.
33. Wei Min Zhang, T. Meier, V. Chernyak, and S. Mukamel. Exciton-migration and three-pulse femtosecond optical spectroscopies of photosynthetic antenna complexes. *J. Chem. Phys.*, 108:7763–74, 1998.
34. S. Krimm and Yasuaki Abe. Intermolecular interaction effects in the amide I vibrations of β polypeptides. *Proc. Nat. Acad. Sci.*, 69:2788–2792, 1972.
35. S. Krimm and W. C. Reisdorf. Understanding normal-modes of proteins. *Faraday Discuss.*, 99:181–197, 1994.
36. S. Mukamel. *Principles of Nonlinear Optical Spectroscopy*. Oxford University Press, New York, 1995.
37. W. M. Zhang, V. Chernyak, and S. Mukamel. Multidimensional femtosecond correlation spectroscopies of electronic and vibrational excitons. *J. Chem. Phys.*, 110:5011, 1999.